Electronic Supplementary Information (ESI)

Enzyme-free amplified detection of miRNA based on target-catalyzed hairpin assembly and DNA-stabilized fluorescent silver nanoclusters

Jinqing Gu,[a] Zhenzhen Qiao,[a] Xiaoxiao He,[a] Yanru Yu,[a] Yanli Lei,[a] Jinlu Tang,[a] Hui Shi,[a,] Dinggeng He,[b,*] and Kemin Wang[a]*

[a] State Key Laboratory of Chemo/Biosensing and Chemometrics, College of Chemistry and Chemical Engineering, College of Biology, Hunan University, Key Laboratory for Bio-Nanotechnology and Molecular Engineering of Hunan Province, Changsha 410082, China.

[b] State Key Laboratory of Developmental Biology of Freshwater Fish, College of Life Sciences, Hunan Normal University, Changsha 410081, China.

[*] E-mail: huishi_2009@hnu.edu.cn; hedinggeng@hnu.edu.cn. Tel/Fax: +86-731-88821566.

Content list

Figures

Optimization of the AP

In order to reduce the background fluorescence of AP and increase the fluorescence triggered by cDNA, the sequence of DNA/BHQ1 was optimized. Here, we regulated the strength of the binding force between DNA/BHQ1 and DNA/AgNCs by changing the length of their complementary sequences, and designed five different sequences of DNA/BHQ1, namely DNA/BHQ1-1, DNA/BHQ1-2, DNA/BHQ1-3, DNA/BHQ1-4 and DNA/BHQ1-5, which were listed in Table S1. These sequences were employed to hybridize with DNA/AgNCs and construct five sets of activatable probes (AP). By measuring and comparing the background fluorescence and response signal of these five sets of probes, we found that the AP consisting of DNA/BHQ1-3 and DNA/AgNCs had the maximal signal-to-background (S/N) ratio (Fig. S1A). Thus, the DNA/BHQ1-3 was used in following experiments. Furthermore, we investigated the effect of the concentration ratio of DNA/BHQ1-3 and DNA/AgNCs on the S/B ratio. As shown in Fig. S1B, the S/B ratio was maximum when the concentration ration of DNA/BHQ1-3 and DNA/AgNCs was 1.5.

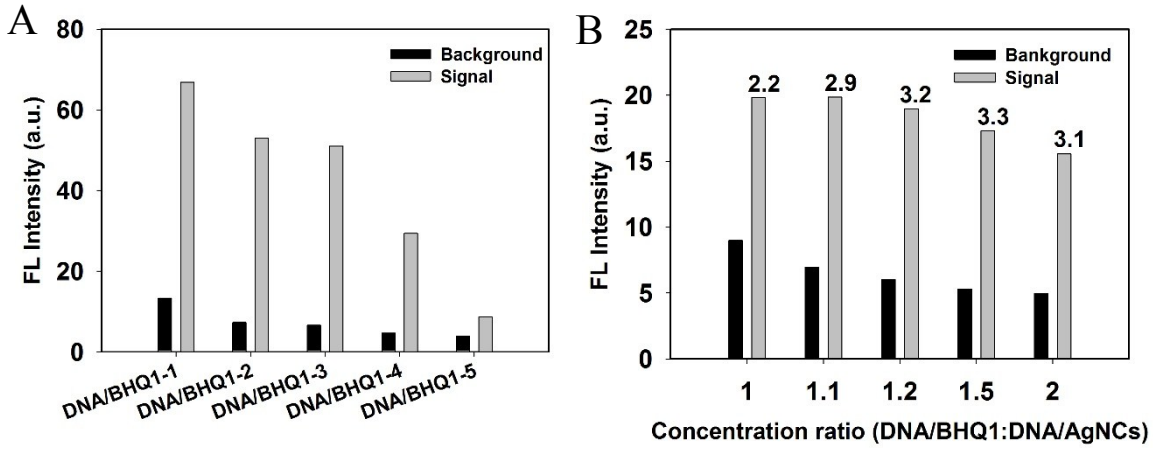

Fig. S1 (A) Fluorescence intensities of AP constructed by different sequences of DNA/BHQ1 with and without cDNA. (B) The S/B ratio of AP at different concentration ratio of DNA/BHQ1-3 and DNA/AgNCs.

Sequence optimization for CHA reaction

CHA reaction was the core of our experimental method, and the main factor affecting the CHA reaction was the sequence design of the hairpin probe H1 and H2. The ideal sequences are that the mixture of H1 and H2 was stable in the absence of target miR-21, whereas the addition of miR-21 can effectively induce the alternate open of H1 and H2. Therefore, three groups of CHA systems were designed, namely CHA-1, CHA-2 and CHA-3 (the detailed sequences shown in Table S1). The fluorescent group FAM was used as the signal source to construct the activatable fluorescent probe (MAP). The fluorescence intensities of MAP in the presence of CHA-1, CHA-2 and CHA-3 systems, respectively, were shown in Fig. S2. Both CHA-1 and CHA-3 systems showed significant target-activated fluorescence signals with a signal-to-background (S/B) ratio of 3.5 and 2, respectively. In contrast, fluorescence signal activated by the CHA-2 system was negligible. Therefore, the sequences of CHA-1 system with higher S/B ratio were chosen for the following experiments.

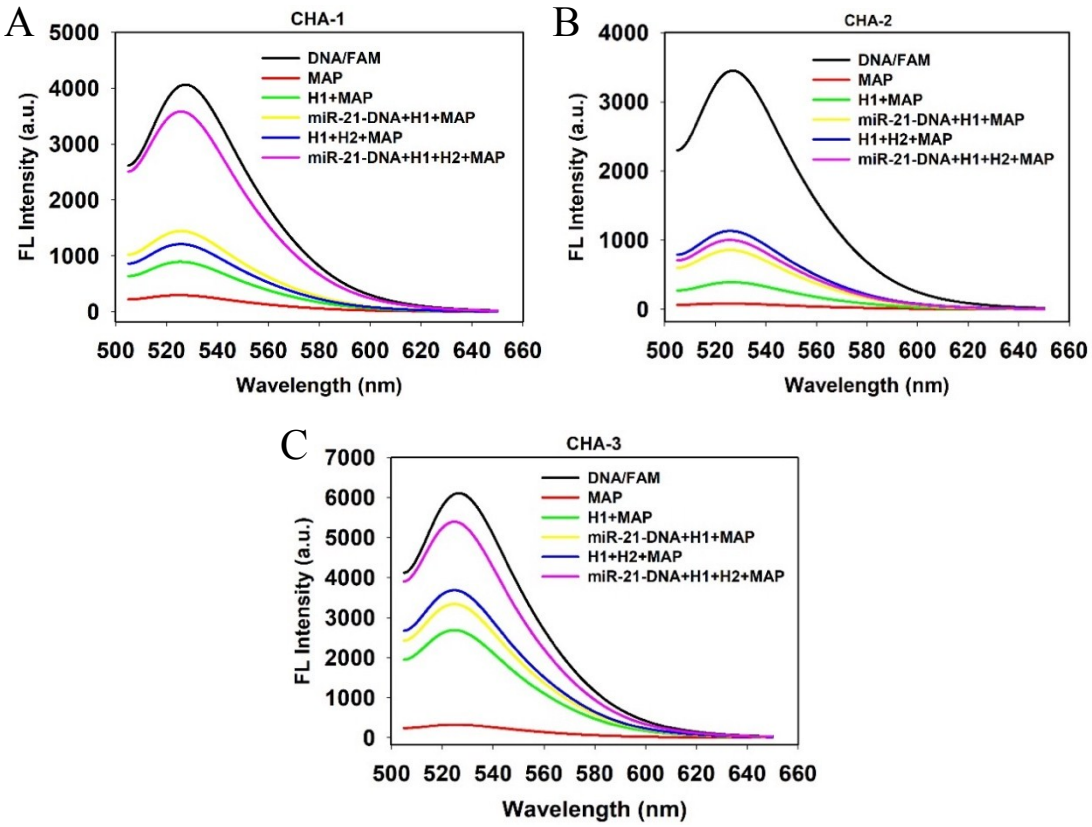

Fig. S2 Fluorescence intensities of the proposed assay with the CHA-1 (A), CHA-2 (B) and CHA-3 systems (C), respectively, by using FAM as the signal source. F represented the fluorescence of the assay with the target miR-21-DNA, and F_0 represented the background fluorescence without target miR-21-DNA.

The proposed sensing assay in different buffers

We investigated the fluorescence intensities of the assay in different buffer solutions (pH 6.5) including PB, Tris-HAc and Tris-HCl. As shown in Fig. S3, the S/B ratios of the assay in the PB, Tris-HAc and Tris-HCl buffers were calculated to be 2.8, 3.5 and 3.2, respectively. In view of the above-mentioned S/B ratios, Tris-HAc (pH 6.5) buffer was used in subsequent experiments.

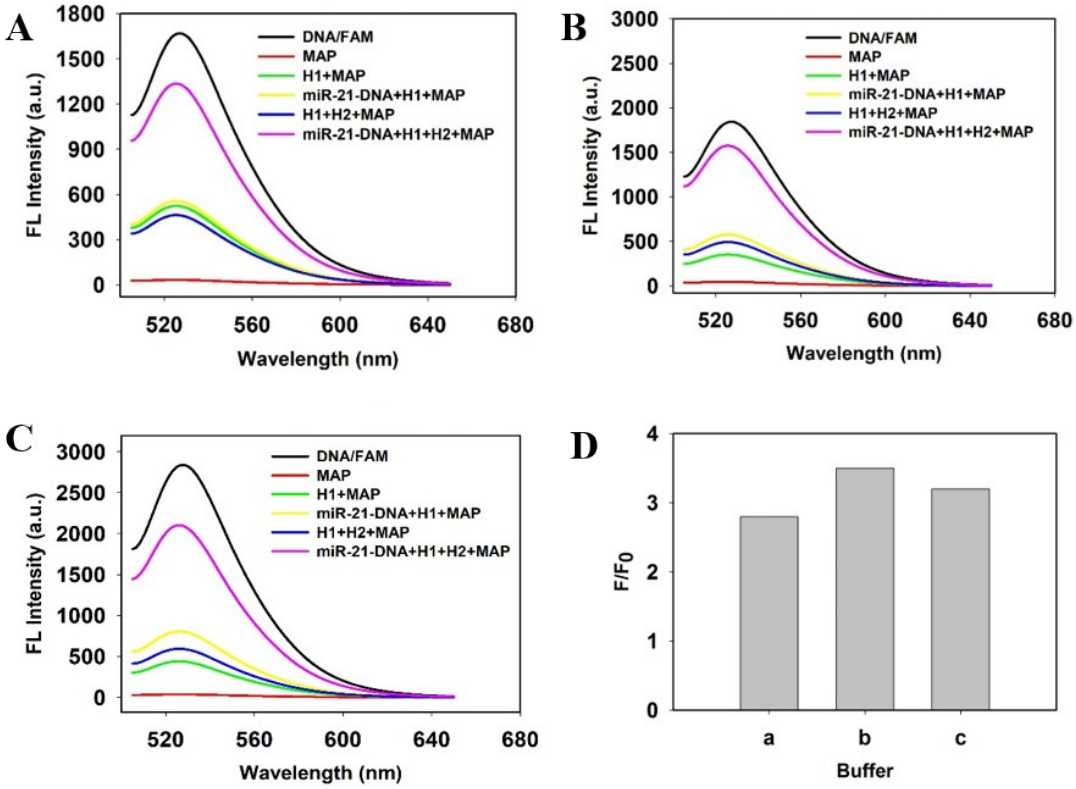

Fig. S3 Fluorescence intensities of the proposed assay in PB buffer (A), Tris-HAc buffer (B) and Tris-HCl buffer (C), respectively. (D) The S/B ratios of the assay in different buffers including PB (a), Tris-HAc (b) and Tris-HCl (c). F represented the fluorescence of the assay with the target miR-21-DNA, and F_0 represented the background fluorescence without target miR-21-DNA.

Optimization of Mg^{2+} concentration

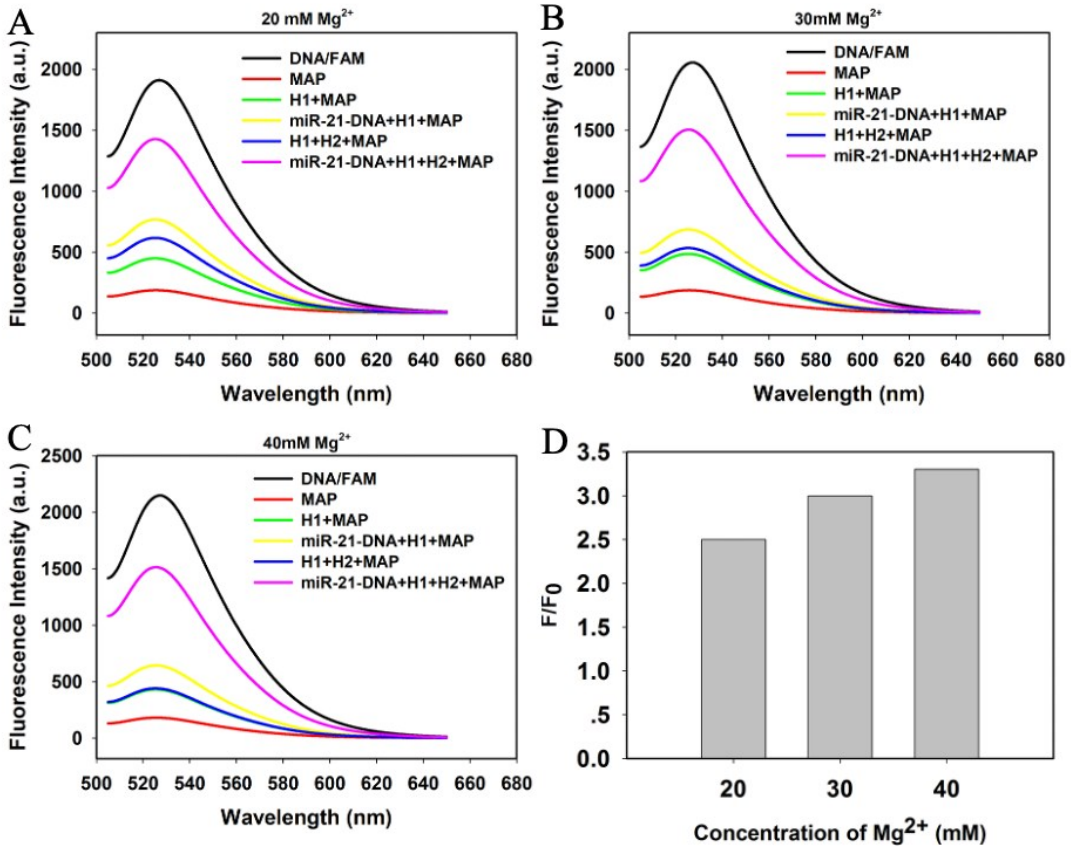

Fig. S4 Fluorescence intensities of the assay in 20 mM Tris-HAc buffer (pH 6.5) in the presence of 20 (A), 30 (B) and 40 mM (C) Mg^{2+} ions, respectively. (D) The S/B ratios of the assay in different concentrations of Mg^{2+} ions. F represented the fluorescence of the assay with the target miR-21-DNA, and F_0 represented the background fluorescence without target miR-21-DNA.

Optimization of miRNA detection conditions

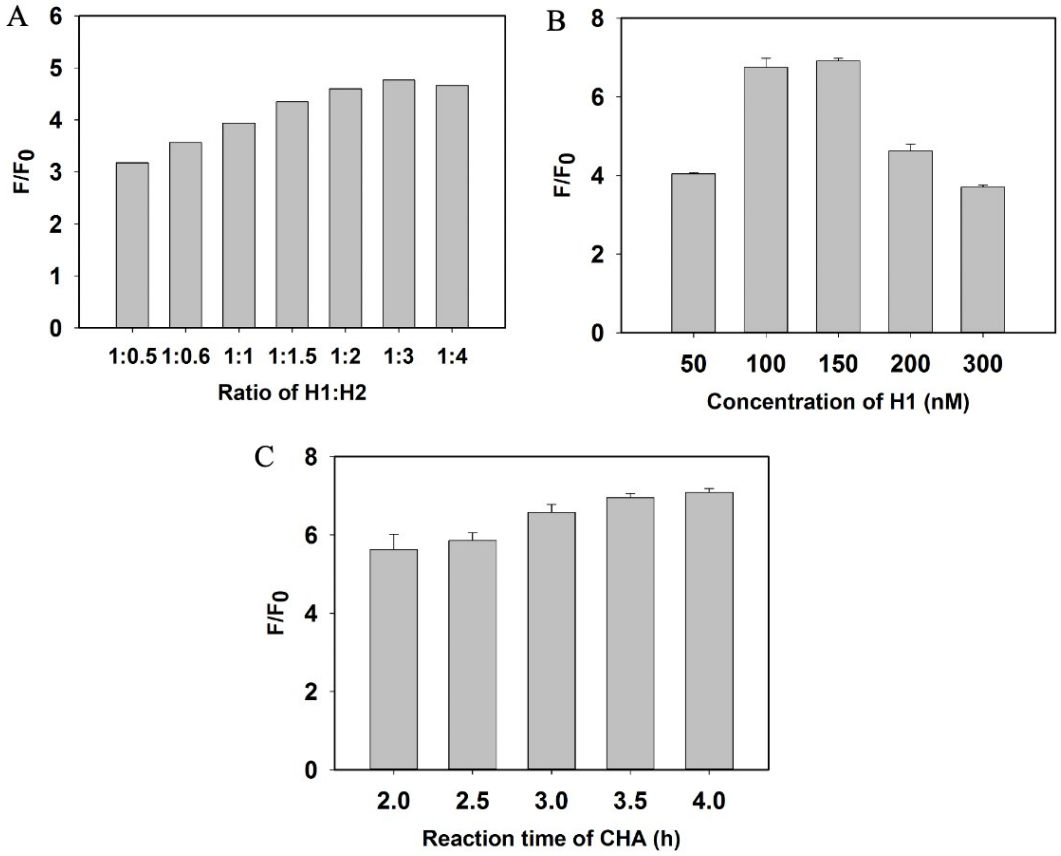

Fig. S5 Optimization of CHA reaction conditions, including concentration ratio of H1 and H2 (A), H1 concentration (B) and reaction time of CHA (C). F represented the fluorescence of the assay with the target miR-21-DNA, and F_0 represented the background fluorescence without target miR-21-DNA.

Selectivity investigation

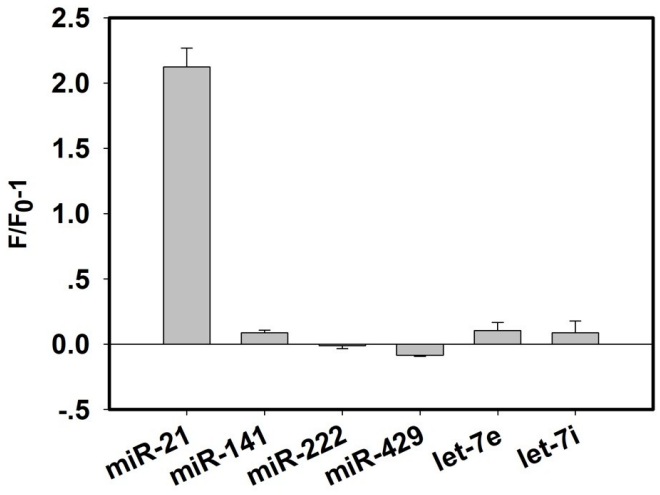

Fig. S6 Selectivity assay. Bars represent the fluorescence intensity ratio (F/F_0-1) upon the different miRNA targets. The concentration of the target miR-21 was 20 nM, and the concentration of the non-target RNA was 200 nM. F_0 and F were the fluorescence signals in the absence and presence of miR-21, respectively.

Table S1. **Oligonucleotide sequences used in this work.**

Names	Sequences (from 5' to 3')
miR-21	UAGCUUAUCAGACUGAUGUUGA
miR-21-DNA	TAGCTTATCAGACTGATGTTGA
DNA/NC	*TACCCCACCCACCCTCCGGGTTTT*CGAGTGCTCTATGACAAGG AGTCTGAT
DNA/FAM	FAM-CGAGTGCTCTATGACAAGGAGTCTGAT
CHA-1-H1	TCAACATCAGTCTGATAAGCTACTACAACTGGCGGGGTAGCT TATCAGACTCCTTGTCATAGAGCAC
CHA-1-H2	TAAGCTACCCCGCCAGTTGTAGTAGCTTATCAGACTCTACAA CTGGCGGGG
CHA-2-H1	TCAACATCAGTCTGATAAGCTACTACAACTGGCGGGGTAGCT TATCAGACTCCTTCTGATAGAGCAC
CHA-2-H2	TAAGCTACCCCGCCAGTTGTAGTAGCTTATCAGACTCTACAA CTGGCGGGG
CHA-3-H1	TCAACATCAGTCTGATAAGCTACATTGGATGCTCTAGCTTATC AGCTGCCTTGTCA TAGAGCAC
CHA-3-H2	TAAGCTAGAGCATCCAATGTAGCTTATCAGACTGCATTGGAT GCTC
DNA/BHQ1-1	TCCTTGTCATAGAGCACTCG-BHQ1
DNA/BHQ1-2	CTTGTCATAGAGCACTCGAAAA-BHQ1
DNA/BHQ1-3	TACTTGTCATAGAGCACTCGAAAA-BHQ1
DNA/BHQ1-4	TCCTTGTCATAGAGCACTCGAAAA-BHQ1
DNA/BHQ1-5	CTCCTTGTCATAGAGCACTCGAAAA-BHQ1
cDNA	ATCAGACTCCTTGTCATAGAGCAC
let-7e	UGA GGU AGG AGG UUG UAU AGU
let-7i	UGA GGU AGU AGU UUG UGC UGU U
miR-141	UAA CAC UGU CUG GUAAAG AUG G
miR-222	AGC UAC AUC UGG CUA CUG GGU CUC
miR-429	UAA UAC UGU CUG GUA AAA CCG U

Note: the italic section represents the template DNA sequence for the synthesis of silver clusters. The miR-21-DNA was the DNA analogue of target miR-21.

Table S2. Comparison of different similar cascade sensing for miRNA detection.

Methods	Target	Detection limit	Linear range	Control target	Ref.
Ratiometric electrochemical biosensor	miR-21	67 aM	0.1 fM-100 pM	single-base mismatched target, two-base mismatched target, non-complementary target	1
Duplex-specific nuclease signal amplification using Taqman probe	miR-141	100 fM	100 pM-100 nM	miR-429, miR-200b, miR-21, let-7d	2
Hybridization chain reaction (HCR)	miR-21	0.25 nM	0.25 nM-25 nM	single-base mismatched RNA, two-base mismatched RNA, random RNA	3
Nucleic acid signal amplification based on strand displacement	miR-21	18 pM	50 pM-10 nM	miRNA-141, miRNA-155, GTP, UTP, CTP	4
WS_2-based duplex-specific nuclease amplification	miR-21	300 fM	1 pM-10 nM	miR-143, miR-141, single-base mismatched miR-21	5
DNA-gold nanoparticle probes	miR-203	5 pM	5 pM-200 pM	miRNA-107, miRNA-9-2, miRNA-338-3p	6
Surface-enhancement Raman scattering (SERS) analysis strategy	miR-21	5 fM	12 fM-18 pM	single-base mismatched miR-21, two-base mismatched miR-21, non-complementary miR-141	7
SERS-based on silver nanorod array	let-7f	28 nM	Not mentioned	miR-218, miR-224	8
Fluorescence method	miR-182	1.7 nM	5 nM-125 nM	one-base mismatched, four-base mismatched, noncomplementary sequences	9
Fluorescence method based on CHA	miR-21	200 pM	200pM-20 nM	miR-141, miR-222, miR-429, let-7e,	**This work**

	let-7i

References-

1. J. Zhang, L.-L. Wang, M.-F. Hou, Y.-K. Xia, W.-H. He, A. Yan, Y.-P. Weng, L.-P. Zeng and J.-H. Chen, *Biosens. Bioelectron*., 2018, **102**, 33-40.
2. B.-C. Yin, Y.-Q. Liu and B.-C. Ye, J. *Am. Chem. Soc.*, 2012, **134**, 5064-5067.
3. Y. Zhang, Z. Chen, Y. Tao, Z. Wang, J. Ren and X. Qu, *Chem. Commun.*, 2015, **51**, 11496-11499.
4. Z.-B. Wen, W.-B. Liang, Y. Zhuo, C.-Y. Xiong, Y.-N. Zheng, R. Yuan and Y.-Q. Chai, *Chem. Commun.*, 2018, **54**, 10897-10900.
5. Q. Xi, D.-M. Zhou, Y.-Y. Kan, J. Ge, Z.-K. Wu, R.-Q. Yu and J.-H. Jiang, *Anal. Chem*., 2014, **86**, 1361-1365.
6. K. Boriachek, M. Umer, M. N. Islam, V. Gopalan, A. K. Lam, N. T. Nguyen and M. J. A. Shiddiky, *Analyst*, 2018, **143**, 1662-1669.
7. D. Ma, C. Huang, J. Zheng, J. Tang, J. Li, J. Yang and R. Yang, *Biosens. Bioelectron*., 2018, **101**, 167-173.
8. J. D. Driskell and R. A. Tripp, *Chem. Commun.*, 2010, **46**, 3298-3300.
9. X. Xia, Y. Hao, S. Hu and J. Wang, *Biosens. Bioelectron*., 2014, **51**, 36–39.